Journal of Applied Electrochemistry **29**: 1475–1479, 1999.

Technical note

Analysis of the presence of different contaminants on the copper electrodeposits morphology obtained from cement copper acid solutions

R. GANA[1], M. FIGUEROA[1], L. KATTAN[1], D. GRANDOSO[2] and M.A. ESTESO[2]*
[1]*Departamento de Química Inorgánica, Facultad de Química, Pontificia Universidad Católica de Chile, Casilla 306, Correo 22, Santiago, Chile;*
[2]*Departamento de Química Física, Universidad de La Laguna, 38204 La Laguna, Tenerife, Spain*
*(*author for correspondence, e-mail: mesteso@ull.es)*

Received 28 September 1998; accepted in revised form 11 May 1999

Key words: cement copper, copper electrodeposits morphology, copper electrorefining

1. Introduction

In previous papers [1–4] a modified anode-support system for the direct electrorefining of cement copper obtained after the leaching of copper oxide minerals from small mines was reported. The optimum operating conditions were presented with regard to the different electrochemical and mechanical variables involved in the process [4]. In this paper a surface morphological study of the copper deposits obtained is presented. These deposits were obtained from copper sulphate solutions contaminated with different elements habitually present in the system during the cementation process used by the small and medium-size mine owners. The copper deposits were produced with an anode-support system consisting of an annular mesh and a vertical rotary cylinder cathode both made in AISI 316 stainless steel by maintaining constant the hydrodynamic and the rest of experimental conditions previously utilized [2].

2. Experimental details

Before each experiment, the AISI 316 stainless steel cylinder (cathode) was consecutively polished up to 600 grain emery paper and with 0.3 μm alumina, washed with detergent, dipped in 10% H_2SO_4 and rinsed with bidistilled water.

Acid solutions prepared from technical grade $CuSO_4.5H_2O$ (150 g dm^{-3}) and H_2SO_4 (50 g dm^{-3}) were used as electrolyte. These solutions were contaminated with As(III) (5–10 g dm^{-3}), Ni(II) (10–20 g dm^{-3}), Zn(II) (10–20 g dm^{-3}), Mg(II) (10–20 g dm^{-3}), Al(III) (10–20 g dm^{-3}), Mn(II) (10–20 g dm^{-3}), Fe(II) (10–40 g dm^{-3}), Sn(II) (0.1–5 g dm^{-3}), SiO_2 (10–20 g dm^{-3}) and Pb(II) + Sb(III) + Ca(II) saturated mixture. These elements were added to the solutions preferentially as sulphate salts because this anion does not interfere with the electrolytic process (for that reason the use of nitrates and chlorides was avoided).

The electrolytic cell used has been described elsewhere [2, 4]. The experimental operating conditions to obtain the deposits were: cathodic current density (j_c) 3 A dm^{-2}, rotation speed (u) 60 rpm and temperature 20 $\pm$ 1 °C. The electrolysis were run for 2 h controlling the cell voltage every 10 min and the current efficiency at the end of each experiment. No pitting corrosion of the anode-support mesh was observed at these operating conditions under the optical microscope (60×). The morphology of the deposits was observed using a scanning electron microscope (SEM) Jeol model JSM 5400. The chemical analysis of the sample surface was performed using both X-ray energy dispersive spectrometry (EDAX) and X-ray photoelectron spectroscopy (XPS) Leybold–Heraeaus model LHS-10, after bombarding the surface with argon ions.

3. Results and discussion

As is well known [5, 6], when pure solutions are utilized, initial copper deposits are homogeneous, with fine grain size, forming a compact layer. For longer deposition time these crystallites grow becoming well formed macrograins of rather uniform size. The growth mechanism results in an adherent, compact, faceted and dendrite-free metallic layer. Nevertheless, when contamined solutions of $CuSO_4$ are used as electrolyte, the morphology of the copper deposits is very different. In Table 1 the maximum permitted technical values for some contaminants in copper electrodeposits are summarized together with the crystallisation type observed.

3.1. *Effect of As(III), Ni(II), Zn(II), Mg(II) and Al(III)*

The presence of any of these contaminant elements in the electrolytic medium during copper deposition, hardly modified the morphology of the deposits, similar as for the deposition of other metals and alloys [7]. On the other hand, the deposits thus obtained exhibited some

Table 1. Maximum permitted technical values in this system for different contaminants in copper electrodeposits and crystallisation type observed for these copper deposits

Contaminant	Concentration /g dm^{-3}	Maximum value permitted/ppm	Crystallization type*
As(III)	5.0	5.0	1
As(III)	10.0	5.0	1–3
Ni(II)	10.0–20.0	3.0	1–3
Zn(II)	10.0	5.0	1–3
Zn(II)	20.0	5.0	1–3–4
Mg(II)	10.0–20.0	3.0	1–3–4
Al(III)	10.0–20.0	–	1–3
Mn(II)	10.0–20.0	3.0	2–4
Fe(II)	10.0–40.0	15.0	2
Sn(II)	0.1	1.0	1–3
Sn(II)	5.0	1.0	2–4
SiO_2	10.0	–	1
SiO_2	40.0	–	2
Pb(II) + Sb(III) + Ca(II)	saturated	–	5

*1. dendritic structure, 2. nodular structure, 3. irregular foliaceous stratiform growth, 4. scoriform intergrain structure, 5. compact pyramidal grains.

stains of different colours (from blue-ish or red-dish until dark brown or black) in which, nevertheless, no differences in both structure and composition were found.

The presence of As(III) in the electrolyte (5–10 g dm^{-3}) made the deposits less uniform and of dendritic structure (Figure 1(a)). The As(III) concentration influenced the dendrite size, which became finer as it increased. The introduction of a cathodic diaphragm [2, 4] into the solution containing 10 g dm^{-3} of As(III) also modified the deposit structure with respect to that obtained in its absence. As observed in Figure 1(b)-A, the dendritic geometry disappeared and a faceted and more compact deposit was found, with well defined grains of different crystallite size indicating a more stable growth mechanism [8]. Nevertheless, some irregular growth with isolated column-like hexagonal-base crystals was detected (Figure 1(b)-B).

The situation was similar in the presence of Ni(II) in the electrolyte, the structure of the deposit obtained being dendritic. In this case, plenty of needle-like irregular structures (Figure 1(c)), randomly distributed and multidirectionally oriented with respect to the substrate surface, was observed.

The presence of Zn(II) led to a dendritic morphology of the metal deposited, similar to that obtained in the presence of As(III), but with the appearance of some isolated hexagonal-base structures. The increase of Zn(II) concentration (10–20 g dm^{-3}) produced an increase in dendrite size. Moreover, a characteristic feature was detected in the intergrain boundaries at the highest concentration. They seemed like scoria, that is, they presented multiple fine pittings (Figure 1(d)) which probably were due to the concurrence of two consecutive processes: a partial codeposition of Zn(II) together with Cu and its ulterior dissolution, as has been reported for the electrodeposition of other metals or alloys [7].

Mg(II) and Al(III) contaminated solutions exhibited a behaviour similar to that of As(III) with the formation of dendritic structures. Nevertheless, in the presence of these contaminants, pyramidal-like structures (Figure 1(e)-A) with hexagonal-base (Figure 1(e)-B) also appeared independently of the contaminant concentration (10–20 g dm^{-3}). These had many forms and sizes and as shown Figure 1(e)-C, they had a foliaceous stratiform growth. In the case of Mg(II) fine pittings at the intergrain boundaries (scoriform appearance as with Zn(II)) also appeared.

In all these cases, EDAX analysis of the deposits only detected pure Cu, although small amounts of oxygen were generally found, indicating some spurious surface copper oxide formation. The XPS spectrum obtained after argon bombarding of the metallic surface confirmed this assumption.

3.2. *Effect of Mn(II) and Fe(II)*

When the solution was contaminated with Mn(II) or Fe(II), the morphology of the metallic deposits was different from that obtained in the above mentioned cases. Here, dendrites were no longer observed. The growth of the crystallites led to the formation of large nodules, mostly of pyramidal form (Figure 1(f)), whose size was not influenced by the contaminant concentration. In the case of Mn(II), scoriform intergrain boundaries were abundantly detected.

EDAX and XPS only detected copper in the deposits.

3.3. *Effect of Sn(II)*

The presence of Sn(II) in the electrolyte led to different deposit characteristics compared to the other contaminants studied. In fact, at the lower concentration used (0.1 g dm^{-3}) the deposits had a rather smooth aspect, although of dendritic morphology, with dendrites mainly of small size. Moreover, some isolated pyramidal-like structures appeared.

Increase in amount of the Sn(II) in the medium (5 g dm^{-3}) changed the structure of the metallic deposit into a nodular one. Nevertheless, the nodules developed were irregular with some flat faces whereas others were brittle (Figure 1(g)). Moreover, in the same way as in the presence of Zn(II), Mg(II) and Mn(II), the intergrain boundaries had fine pittings (scoria-like) when the concentration of Sn(II) was high (5 g dm^{-3}).

EDAX analysis of these deposits detected pure copper when the contaminant concentration was 0.1 g dm^{-3}, but showed the inclusion of tin in the deposits when the concentration of the contaminant in the liquid phase increased to 5 g dm^{-3}. In fact, EDAX spectrum of the metal deposit base showed the existence of 3.63% of tin and 7.46% of oxygen, which would be incorporated to the Cu deposit as a non stoichiometric stannic oxide

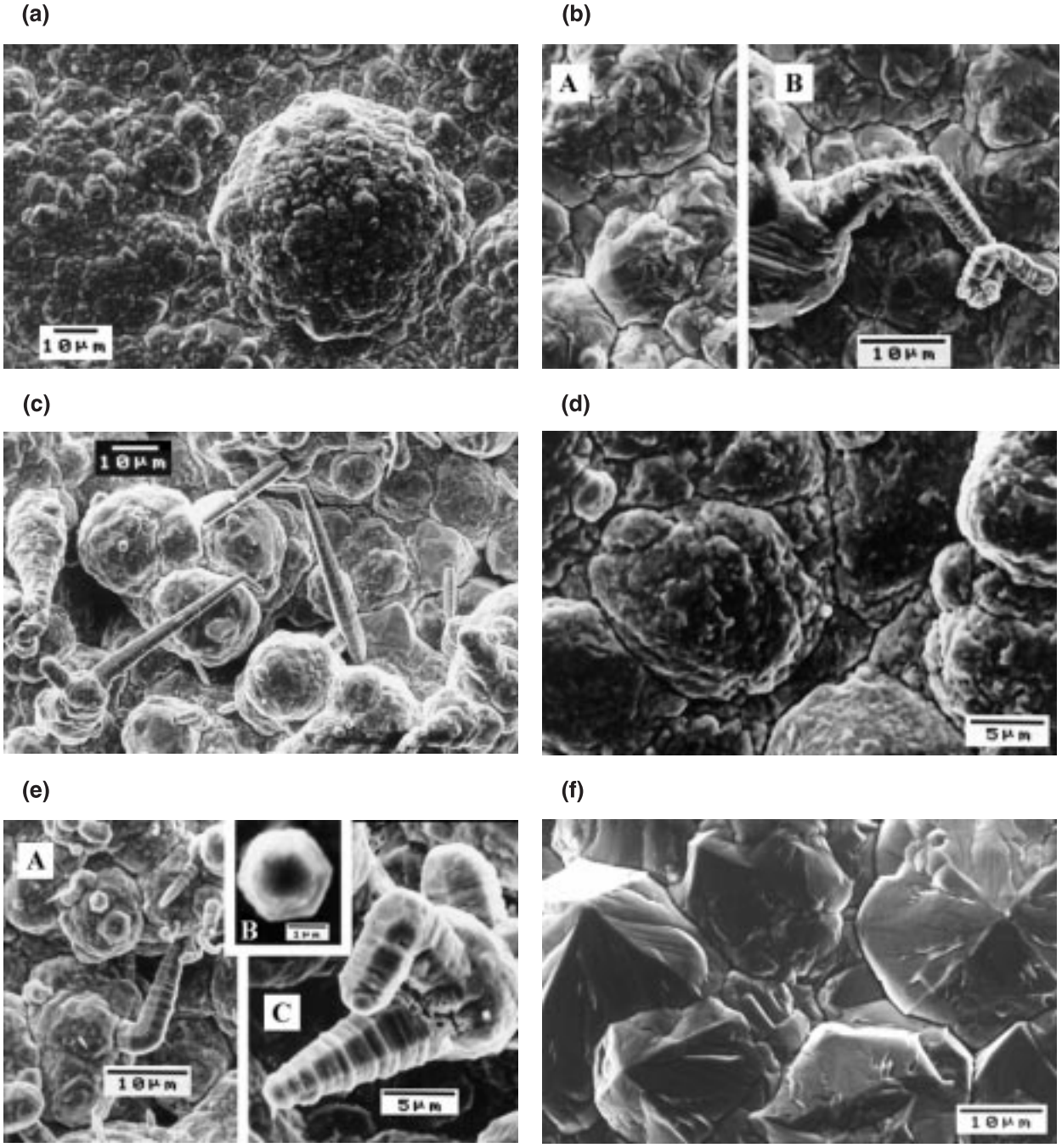

Fig. 1. SEM micrographs of the morphology for the deposits obtained, after 2 h of electrolysis, from an acid solution contaminated with: (a) 5 g dm^{-3} As(III); (b) 10 g dm^{-3} As (III), by using a cathodic diaphragm into the solution: (A) base deposit, (B) irregular growth observed; (c) 20 g dm^{-3} Ni(II); (d) 20 g dm^{-3} Zn(II); (e) Mg(II): (A) 10 g dm^{-3}, (B) hexagonal-base of the structures obtained with 10 g dm^{-3} of the contaminant, (C) 20 g dm^{-3}; (f) 10 g dm^{-3} Fe(II); (g) 5 g dm^{-3} Sn(II); (h)SiO_2: (A) 10 g dm^{-3}, (B) 20 g dm^{-3}; (i) Pb(II) + Sb(III) + Ca(II) saturated mixture.

aggregate. The spectra for the nodule walls (on the flat and on the brittle ones) also revealed, in all cases, the presence of different amounts of Sn (0.9–8.0%) and O (3.3–8.8%) codeposited with Cu, which indicates that they were incorporated under stannous-stannic oxides mixture form and even as free Sn.

This was confirmed by XPS spectroscopy using either Al or Mg filaments. The perfectly defined Sn 3d absorption band (with binding energies of 484.0 eV for Sn $3d_{5/2}$, and 492.2 eV for Sn $3d_{3/2}$), after bombardment of the deposit with argon ions, showed the presence of 3.7 mass % of Sn and 11.4 mass % of O. XPS analysis was repeated for the surface near to the AISI 316 stainless steel cathode (inner surface) in order to elucidate whether the presence of Sn was superficial or in depth. The results showed evidence of a codeposition phenomenon of the Sn (as oxide) all along the electrodeposition process. Nevertheless, due to the fact that for this inner surface of the deposit the concentration of Sn (2.2%) was less than that found at

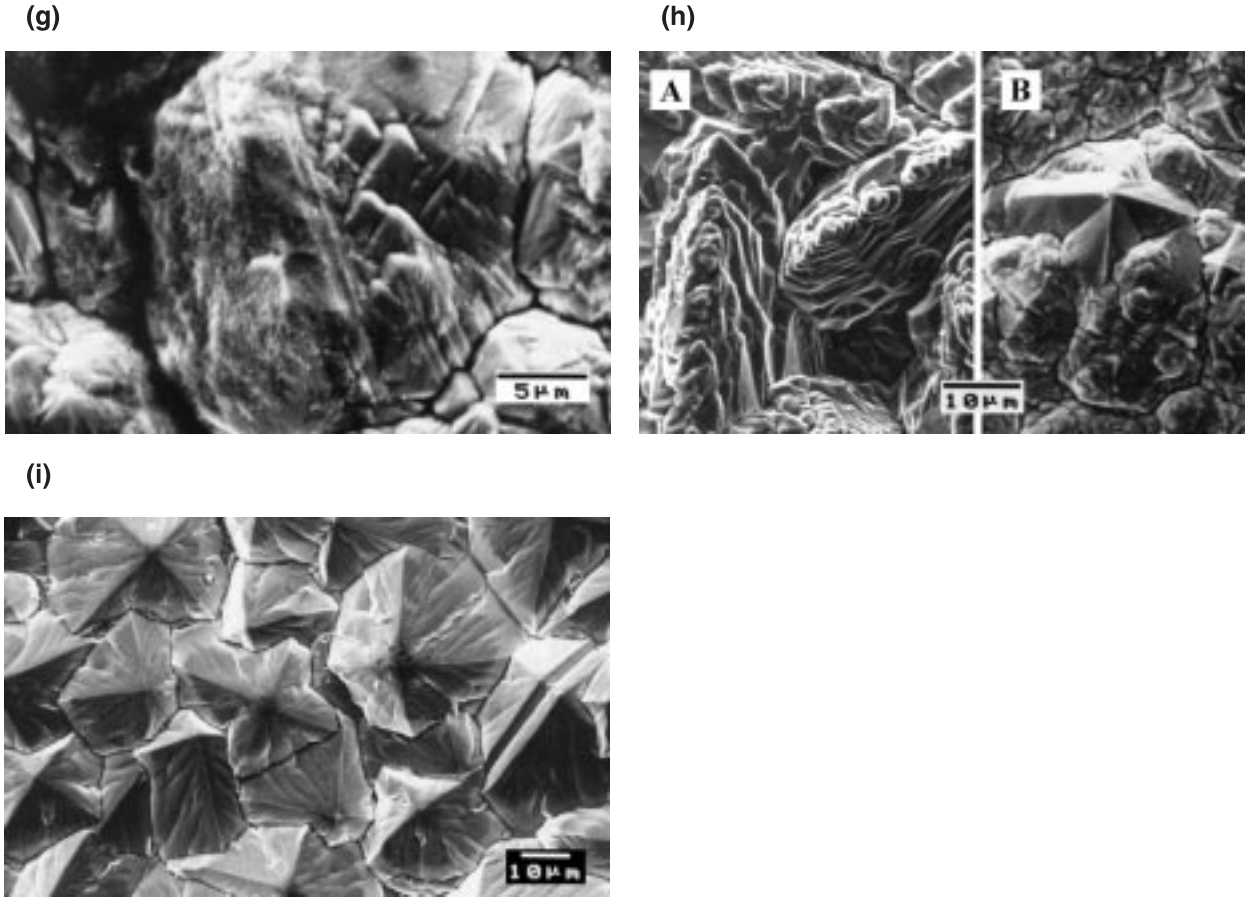

Fig. 1. Continued, g–i.

the outer surface, it can be assumed that a partial redissolution of this contaminant took place, which explains the appearance of pitting at the intergrain boundaries. Using a similar argument, the above mentioned scoria-like structures observed in the presence of Zn(II), Mg(II) and Mn(II) contaminants can also be explained.

The use of a cathodic diaphragm in the solution did not change the morphology of the deposits, but EDAX and XPS analysis showed codeposited Sn with Cu. This behaviour can be explained by taking into account that Sn forms a colloidal metastannic acid in acid solution.

3.4. *Effect of SiO_2*

The morphology of the electrodeposits in the presence of SiO_2 was very sensitive to the content of the contaminant in the solution but, in any case, they completely differed from those observed up to now. Thus at 10 g dm^{-3} structures like flower-leaf (dendrites), randomly oriented, were found (Figure 1(h)-A). When the concentration increased (up to 20 g dm^{-3}) the structure of the deposits improved, since these structures became more compact with small rounded grains together with a few nodules (Figure 1(h)-B). At higher SiO_2 concentration (40 g dm^{-3}) the morphology of the deposits stayed the same, although it seemed to be more compact.

In all cases, EDAX and XPS analysis did not detect peaks of elements other than Cu.

3.5. *Effect of Pb(II) + Sb(III) + Ca(II) saturated mixture*

The deposits had zones of different colours (intense blue, red-dish and dark brown) but no differences in both morphology and structure were observed compared to the rest of the metallic deposits. The morphology was quite uniform, dendrite-free, consisting of intermixed pyramidal grains, that were very well outlined (Figure 1(i)) and suggested good adherence.

In a similar way to most of the contaminants studied here, only copper was detected by EDAX and XPS analysis.

4. Conclusions

The morphology of the electrodeposits of Cu from $CuSO_4$ acid solutions were definitely influenced by the presence of the contaminants investigated. In the presence of As(III), Ni(II), Zn(II), Mg(II), Al(III) and low concentration of Sn(II) (0.1 g dm^{-3}) and SiO_2 (10 g dm^{-3}) they were of dendritic structure with dendrite size generally depending on the contaminant concentration present in the electrolyte solution.

When the contaminants were Mn(II), Fe(II), and high concentration of Sn(II) (5 g dm^{-3}) and SiO_2 (from 20 g dm^{-3}) this morphology became nodular.

On the one hand, irregular column growth (needle-like, pyramidal-like, hexagonal-base) mainly of foliaceous stratiform type were observed in the presence of As(III), Ni(II), Zn(II), Mg(II), Al(III) and Sn(II) contaminants. On the other hand, fine pittings in the grain boundaries were detected for Zn(II), Mg(II), Mn(II) and Sn(II) which can be attributed to the occurrence of a codeposition process of the contaminant elements together with Cu, followed by a redissolution (oxidation) of the deposited contaminants.

The morphology of the deposit obtained in the presence of Pb(II) + Sb(III) + Ca(II) saturated mixture was different from the rest of those obtained here, giving large intermixed pyramidal grains which were well outlined and showed adherent appearance.

In all cases except that of 5 g dm^{-3} of Sn, EDAX and XPS analysis detected only copper. When Sn(II) was present at the highest concentration tested, it codeposited with Cu mainly in the stannous oxide form. For this reason it is very important to avoid the presence of tin in scrap utilized in cementation process of copper (can coatings, weldings, etc.).

Acknowledgements

The authors are grateful for support from the Fondo Nacional de Desarrollo Científico y Tecnológico (FONDECYT) and from the Dirección de Investigación de la Pontificia Universidad Católica de Chile (DIUC). The authors thank Ms Montserrat Hernández-Barrera for her help in the final revision of the linguistic aspects of the English text.

References

1. R. Gana, M. Figueroa, L. Kattan, J.M. Sánchez and M.A. Esteso, *J. Appl. Electrochem.* **25** (1995) 240.
2. R. Gana, M. Figueroa, L. Kattan, I. Moller and M.A. Esteso, *J. Appl. Electrochem.* **25** (1995) 1052.
3. M. Figueroa, R. Gana, L. Kattan , S. Méndez and L. Palma, *J. Appl. Electrochem.* **27** (1997) 99.
4. R. Gana and M. Figueroa, *Hydrometallurgy* **47** (1998) 149.
5. L. Bonou, M. Eyrand and J. Crousier, *J. Appl. Electrochem.* **24** (1994) 906.
6. R. Rashkov and C. Nanev, *J. Appl. Electrochem.* **25** (1995) 603.
7. H.M. Wang and T.J. O'Keefe, *J. Appl. Electrochem.* **24** (1994) 900.
8. A.N. Baraboshkin, 'Electrocristalizatsya Metallov iz Rasplavlennish Solei', (Nauka, Moscow, 1976).